Article

Bioresponsive Hydrogel Microlenses

Jongseong Kim, Satish Nayak, and L. Andrew Lyon

J. Am. Chem. Soc., **2005**, 127 (26), 9588-9592• DOI: 10.1021/ja0519076 • Publication Date (Web): 10 June 2005

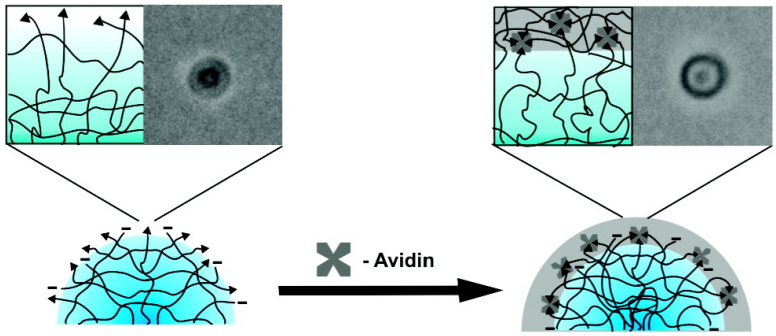

More About This Article

Additional resources and features associated with this article are available within the HTML version:

- Supporting Information
- Links to the 28 articles that cite this article, as of the time of this article download
- Access to high resolution figures
- Links to articles and content related to this article
- Copyright permission to reproduce figures and/or text from this article

View the Full Text HTML

J|A|C|S
ARTICLES
Published on Web 06/10/2005

Bioresponsive Hydrogel Microlenses

Jongseong Kim, Satish Nayak, and L. Andrew Lyon*

Contribution from the School of Chemistry and Biochemistry, Georgia Institute of Technology, Atlanta, Georgia 30332-0400

Received March 24, 2005; E-mail: lyon@chemistry.gatech.edu

Abstract: We report investigations of bioresponsive hydrogel microlenses as a new protein detection technology. Stimuli-responsive poly(*N*-isopropylacrylamide-*co*-acrylic acid) (pNIPAm-*co*-AAc) microgels have been synthesized via free-radical precipitation polymerization. These hydrogel microparticles were then functionalized with biotin via EDC coupling. Hydrogel microlenses were prepared from the particles via Coulombic assembly onto a silane-modified glass substrate. Arrays containing both pNIPAm-*co*-AAc microgels (as an internal control) and biotinylated pNIPAm-*co*-AAc microgels were then used to detect multivalent binding of both avidin and polyclonal anti-biotin. Protein binding was determined by monitoring the optical properties of the microlenses using a brightfield optical microscopy technique. The microlens method is shown to be very specific for the target protein, with no detectable interference from nonspecific protein binding. Finally, the reversibility of the hydrogel microlens assay has been studied in the case of anti-biotin to determine the potential application of the microlens assay technology in a displacement-type assay. These results suggest that the microlens method may be an appropriate one for label-free detection of proteins or small molecules via displacement of tethered protein−ligand pairs.

Introduction

Over the past decade, a number of applications involving stimuli-sensitive hydrogels have arisen due to the great potential for hydrogels as matrices, actuators, and transducers.[1−6] Many of these hydrogels have been thermoresponsive, which undergo a reversible phase separation at the lower critical solution temperature (LCST) or upper critical solution temperature (UCST) of the polymer.[7−11] It has been reported that specifically engineering such hydrogels with additional functionalities can result in hydrogels that are responsive to stimuli, such as pH, ionic strength, photon flux, and biomolecular binding events.[12−17] These additional stimuli-responsive characteristics make them useful for numerous applications, such as controlled drug release,[18−20] tissue regeneration,[1] surface patterning,[3,21] microfluidic flow control,[22−24] tunable optics,[4,25,26] molecular switches,[2] and sensing transducers.[4,27,28]

Our group has recently shown that poly(*N*-isopropylacrylamide-*co*-acrylic acid) (pNIPAm-*co*-AAc) microgels can be used to fabricate dynamically tunable microlens arrays.[25,26,29] Such tunable microlens arrays are easily assembled on an aminopropyltrimethoxysilane (APTMS)-functionalized glass substrate via common electrostatic interactions. The optical properties of these hydrogel-based microlenses can be tuned by different stimuli, such as temperature, pH, and photons, as a result of the responsivity of the network to those stimuli.[25,26] Furthermore, the lens-like structure enables us to visualize subtle changes in gel swelling at the microscale using a simple optical microscope setup. In this contribution, we describe the use of this microlensing methodology to visualize the modulation of gel swelling via protein−ligand interactions. This construct represents a new

(1) Lutolf, M. P.; Lauer-Fields, J. L.; Schmoekel, H. G.; Metters, A. T.; Weber, F. E.; Fields, G. B.; Hubbell, J. A. *Proc. Natl. Acad. Sci. U.S.A.* **2003**, *100* (9), 5413−5418.
(2) Shimoboji, T.; Larenas, E.; Fowler, T.; Kulkarni, S.; Hoffman, A. S.; Stayton, P. S. *Proc. Natl. Acad. Sci. U.S.A.* **2002**, *99* (26), 16592−16596.
(3) Hu, Z.; Chen, Y.; Wang, C.; Zheng, Y.; Li, Y. *Nature* **1998**, *393* (6681), 149−152.
(4) Holtz, J. H.; Asher, S. A. *Nature* **1997**, *389* (6653), 829−832.
(5) Liu, L.; Li, P.; Asher, S. A. *Nature* **1999**, *397* (6715), 141−144.
(6) Langer, R.; Tirrell, D. A. *Nature* **2004**, *428* (6982), 487−492.
(7) Pelton, R. *Adv. Colloid Interface Sci.* **2000**, *85*, 1−33.
(8) Tanaka, T.; Fillmore, D. J. *J. Chem. Phys.* **1979**, *70*, 1214−1218.
(9) Dusek, K.; Patterson, K. *J. Polym. Sci., Polym. Phys. Ed.* **1968**, *6* (7), 1209−1216.
(10) Heskins, M.; Guillet, J. E. *J. Macromol. Sci. Chem.* **1968**, *A2*, 1441−1455.
(11) Arotcarena, M.; Heise, B.; Ishaya, S.; Laschewsky, A. *J. Am. Chem. Soc.* **2002**, *124* (14), 3787−3793.
(12) Gan, D.; Lyon, L. A. *J. Am. Chem. Soc.* **2001**, *123* (31), 7511−7517.
(13) Nayak, S.; Lee, H.; Chmielewski, J.; Lyon, L. A. *J. Am. Chem. Soc.* **2004**, *126* (33), 10258−10259.
(14) Nayak, S.; Lyon, L. A. *Chem. Mater.* **2004**, *16* (13), 2623−2627.
(15) Wang, C.; Flynn, N. T.; Langer, R. *Adv. Mater.* **2004**, *16* (13), 1074−1079.
(16) Wang, C.; Stewart, R. J.; Kopecek, J. *Nature* **1999**, *397* (6718), 417−420.
(17) Miyata, T.; Asami, N.; Uragami, T. *Nature* **1999**, *399* (6738), 766−769.
(18) Serpe, M. J.; Yarmey, K. A.; Nolan, C. M.; Lyon, L. A. *Biomacromolecules* **2005**, *6* (1), 408−413.
(19) Nolan, C. M.; Serpe, M. J.; Lyon, L. A. *Biomacromolecules* **2004**, *5* (5), 1940−1946.
(20) Kikuchi, A.; Okano, T. *Adv. Drug Delivery Rev.* **2002**, *54* (1), 53−77.
(21) Suh, K. Y.; Langer, R.; Lahann, J. *Adv. Mater.* **2004**, *16* (16), 1401−1405.
(22) Yu, Q.; Bauer, J. M.; Moore, J. S.; Beebe, D. J. *Appl. Phys. Lett.* **2001**, *78* (17), 2589−2591.
(23) Beebe, D. J.; Moore, J. S.; Bauer, J. M.; Yu, Q.; Liu, R. H.; Devadoss, C.; Jo, B.-H. *Nature* **2000**, *404* (6778), 588−590.
(24) Arndt, K.-F.; Kuckling, D.; Richter, A. *Polym. Adv. Technol.* **2000**, *11* (8−12), 496−505.
(25) Kim, J.; Serpe, M. J.; Lyon, L. A. *Angew. Chem., Int. Ed.* **2005**, *44*, 1333−1336.
(26) Kim, J.; Serpe, M. J.; Lyon, L. A. *J. Am. Chem. Soc.* **2004**, *126* (31), 9512−9513.
(27) Yoshimura, I.; Miyahara, Y.; Kasagi, N.; Yamane, H.; Ojida, A.; Hamachi, I. *J. Am. Chem. Soc.* **2004**, *126* (39), 12204−12205.
(28) Lee, M.-C.; Kabilan, S.; Hussain, A.; Yang, X.; Blyth, J.; Lowe, C. R. *Anal. Chem.* **2004**, *76* (19), 5748−5755.
(29) Serpe, M. J.; Kim, J.; Lyon, L. A. *Adv. Mater.* **2004**, *16* (2), 184−187.

10.1021/ja0519076 CCC: $30.25

Scheme 1. Conceptual Representation of the Hydrogel Microlens Assay[a]

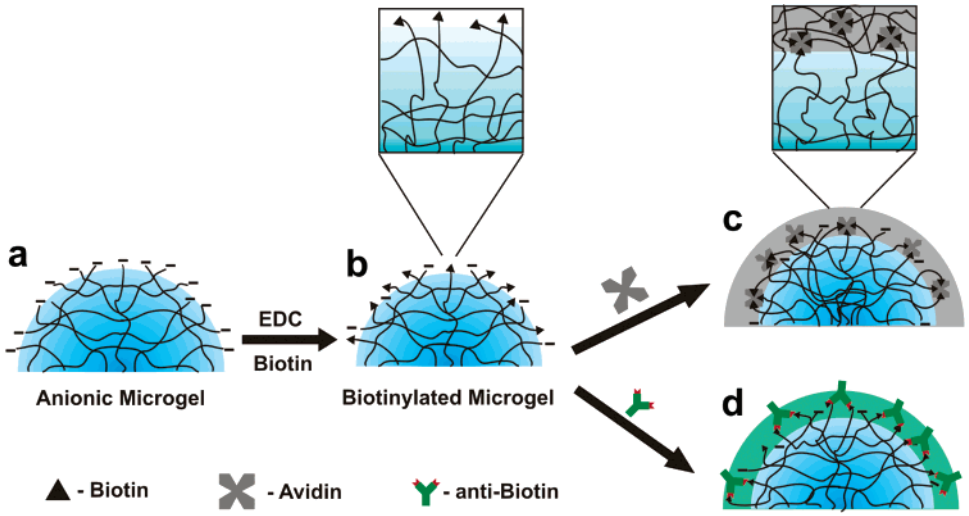

[a] (a) pNIPAm-*co*-AAc hydrogel microparticles synthesized by aqueous free-radical precipitation polymerization method. (b) Biotinylation of pNIPAm-*co*-AAc hydrogel microparticles via EDC coupling. (c) Formation of cross-links in the hydrogel by multivalent binding of avidin to biotin on the hydrogel microlenses. (d) Cross-link formation in the hydrogel microlens by multivalent binding of anti-biotin to biotin on the hydrogel microlenses.

method of visualizing protein assays wherein the gel substrate itself is also the transducer element.

The particular issue in developing a biological assay is achieving not only high selectivity to the target molecules but also simplicity in fabrication. An inexpensive assay technique that is generalizable to a wide range of different affinity pairs with high selectivity would increase the potential for the use of the technique in many applications, such as protein assays, drug screening, chemical sensing, and the detection of genetic defects, such as single nucleotide polymorphisms. In the present research, we have developed a new protein assay method by utilizing ligand-functionalized hydrogels, which simultaneously associate with the protein of interest and report on the binding event. In particular, the technique described here is free from false signals due to nonspecific binding and could be used for very complex mixtures by employing the inherent advantage of a displacement-type assay scheme.

Results and Discussion

The main strategy in this work is to utilize the biotinylated pNIPAm-*co*-AAc hydrogel microparticles as both the protein recognizing and transducing material (Scheme 1). In this strategy, a portion (~50%) of the acid groups of the microgels are conjugated to the biotin ligand via EDC coupling. These biotinylated microgels then interact with multivalent proteins (avidin and anti-biotin), which form additional cross-links between polymer chains in the network. Such a cross-linking event results in the change in the equilibrium swelling volume of the microgel and, hence, an increase in the local refractive index (RI) of the microgel. Our group has recently shown that the optical properties of the hydrogel microlenses are dependent on the refractive index (RI) contrast between the hydrogel and the surrounding medium.[25,26] Also, microlenses formed from pH- and temperature-responsive gels are able to project images of different fidelities in response to pH and temperature changes, respectively.

To investigate the potential utility of hydrogel microlenses in this protein assay system, we prepared substrates containing a random, binary distribution of microlenses, where both pNIPAm-*co*-AAc microlenses and biotinylated pNIPAm-*co*-AAc microlenses are present in approximately equal number densities. Under the deposition conditions used, a submonolayer coverage of microlenses is obtained, which allows for imaging of individual microlens optical properties without interference from adjacent particles. Both modified and unmodified microlenses were used to prepare these samples such that the unmodified microlens can act as an internal control and reference state. The microlenses were then exposed to various concentrations of avidin solutions by introduction of 150 μL of the proper solution into the void space of a microlens array/silicone gasket/coverslip sandwich assembly. The effects of avidin concentration on the optical properties of the microlenses are shown in Figure 1. It is interesting to note that only the biotinylated hydrogel

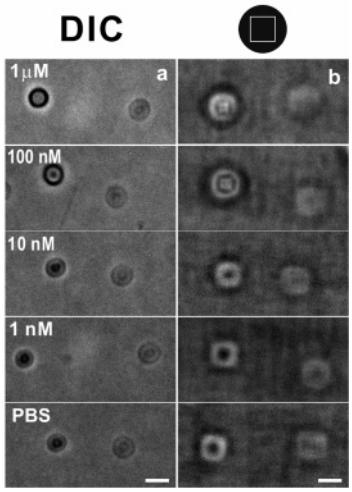

Figure 1. Dependence of microlens swelling in 10 mM PBS buffer solution as a function of avidin concentration at room temperature. (a) DIC microscopy images of substrate-bound pNIPAm-*co*-AAc hydrogels (right element in each panel) and biotinylated pNIPAm-*co*-AAc hydrogels (left element in each panel) at the indicated avidin concentrations. (b) Projection of the single square pattern (top right) through the hydrogel microlenses under the same conditions as described for column a. As the avidin concentration increases, only the biotinylated hydrogel microlenses form dark circles in DIC images (a) and show modulation of the square images in projection mode (b). Note that 150 μL of each solution was used for this experiment (100 nM is equivalent to 15 pmol of avidin). The scale bar is 2 μm.

microlenses (left elements in each panel) show a difference in appearance in the differential interference contrast (DIC)[30] images as the avidin concentration is increased, with the most marked difference being the formation of the dark circle at the particle periphery (Figure 1a). The nonbiotinylated microlenses (right elements in each panel) do not show any apparent change at different concentrations of avidin. In Figure 1b, the biotinylated microlenses exhibit a large change in image formation (white square) at 100 nM avidin (equivalent to 15 pmol of protein), while the nonbiotinylated hydrogel microlenses show a weak, poorly focused image over the entire range of the avidin concentrations. The change in lens projection observed for the biotinylated lenses appears to be the formation of a double image, where the periphery of the particle appears bright, while a small, more tightly focused square appears at the center of the microlens. These phenomena are due to the local RI change of the biotinylated hydrogels caused by the formation of biotin−avidin networking on the surface at a critical avidin concentration. The higher RI decreases the effective focal length of the microlens, hence creating a smaller, more tightly focused image of the white square pattern. It may also be the case that the higher refractive index at the microlens surface causes an increase in light scattering, which may be the origin of the bright appearance of the particle periphery. Regardless of the detailed origins of the image formation, it is clear that the ligand-modified lenses are sensitive to protein binding and directly report on that binding through a change in both microlens appearance (Figure 1a) and microlens performance (Figure 1b). Also, note that the biotinylated hydrogel microlenses have very different optical properties (focal lengths) than the nonbiotinylated microlenses before introduction of the protein (e.g., in PBS only). This arises from the decrease in the number of acidic sites in the biotinylated microgels, which decreases the equilibrium swelling volume and, hence, increases the RI of the microlens.

In designing any affinity-based assay system, mediation of nonspecific adsorption and enhancement of selectivity are two of the key figures of merit. Thus, fluorescence microscopy was used to investigate specific biotin−avidin binding to the hydrogel microlenses (Figure 2a and b). Note that the avidin and hydrogels are labeled by fluorescent chromophores with red (Texas red) and green (fluorescein) emission spectra, respectively. The appearance of the red fluorescence at the periphery of the left element in panel a confirms that the avidin only binds to the surface of the biotinylated hydrogel microlens. Interestingly, there is no discernible nonspecific adsorption to the nonbiotinylated hydrogel microlens at the same solution avidin concentration (right element in panel a). Nonbiotinylated microlenses also do not show any nonspecific adsorption when they are present alone on the substrate (data not shown). Note that in PBS buffer, both microlenses display only green fluorescence due to fluorescein, although the biotinylated microlens appears to have fluorescence intensity that is weaker than that of the nonbiotinylated one. This may be due to a difference in the photobleaching rate between the two particles, or it may be that biotin acts as a quencher when placed in close proximity to fluorescein. Finally, brightfield transmission microscopy was used to scrutinize the selectivity of these assay systems by exposing the biotinylated microlenses to a solution of anti-avidin (panels c and d). The DIC images of the hydrogel microlenses are unchanged by the presence of anti-avidin at a solution concentration of 730 nM (equivalent to 110 pmol) as compared to images acquired in PBS buffer solution.

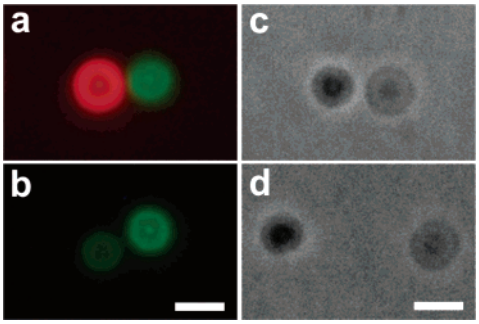

Figure 2. Fluorescence microscopy images of hydrogel microlenses in (a) 1 μM avidin in 10 mM PBS and (b) a 10 mM PBS buffer solution. Note that the microgel is labeled with 4-acrylamidofluorescein (green), and avidin (red) is conjugated with Texas red. Biotin−avidin binding is observed only on the biotinylated microgel (left element in each panel) and not on the nonbiotinylated microgel (right element in each panel) at the tested avidin concentration. (c) DIC microscopy image of the bare microgels (right element in each panel) and the biotinylated microgels (left element in each panel) in 730 nM anti-avidin in 10 mM PBS and (d) 10 mM PBS buffer solution. There is no discernible change on DIC images due to the nonspecific adsorption of anti-avidin. Note that 150 μL of each solution was used for this experiment (1 μM is equivalent to 150 pmol). The scale bar is 2 μm.

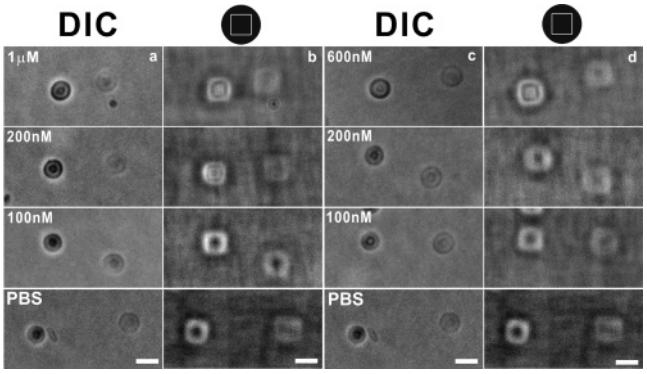

Figure 3. Sensitivity of the hydrogel microlens assay to the number of the active binding sites on avidin. The different number of the active sites were prepared by equilibrating avidin with different stoichiometric ratios of biotin. (a) DIC images of the hydrogel microlenses exposed to 1:1 biotin:avidin solutions in 10 mM PBS buffer as a function of total avidin concentration. (b) Projection of the single square pattern (top) through the hydrogel microlenses under the same conditions as described for column a. (c) DIC images of the hydrogel microlenses exposed to 2:1 biotin:avidin solutions in 10 mM PBS buffer as a function of total avidin concentration. (d) Projection of the single square pattern (top) through the hydrogel microlenses under the same conditions as described for column c. Note that 150 μL of each solution was used for this experiment (100 nM is equivalent to 15 pmol). The scale bar is 2 μm.

As described above, we propose that the [avidin]-dependent microlens response is caused by an increase in the network cross-link density, due to the ability of avidin to bind up to 4 equiv of biotin. To prove the requirement of multivalent binding, we investigated the sensitivity of the microlens assay to avidin that had been equilibrated with different amounts of free biotin. Figure 3 shows the DIC (panels a and c) and lens projection (panels b and d) images of the hydrogel microlenses exposed to avidin solutions pre-equilibrated with 1 (panels a and b) or 2 (panels c and d) equiv of biotin. Because of the extraordinarily

(30) Murphy, D. B. *Fundamentals of Light Microscopy and Electronic Imaging*; Wiley-Liss: New York, 2001.

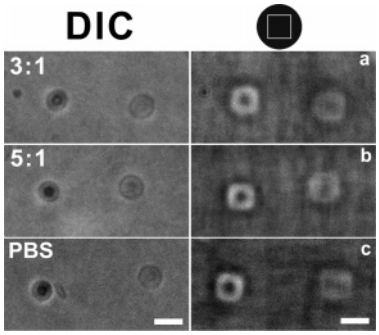

Figure 4. Effects of the monovalent binding and the nonspecific adsorption. (Left column) DIC images of the hydrogel microlenses and (right column) projected square pattern images through the hydrogel microlenses in 1 μM biotin-equilibrated avidin solutions with the ratio of (a) 3:1, (b) 5:1 biotin:avidin, and (c) 10 mM PBS buffer. The bare microgels (right element in each panel) and the biotinylated microgels (left element in each panel) are unchanged under these conditions. Note that 150 μL of each solution was used for this experiment (100 nM is equivalent to 15 pmol). The scale bar is 2 μm.

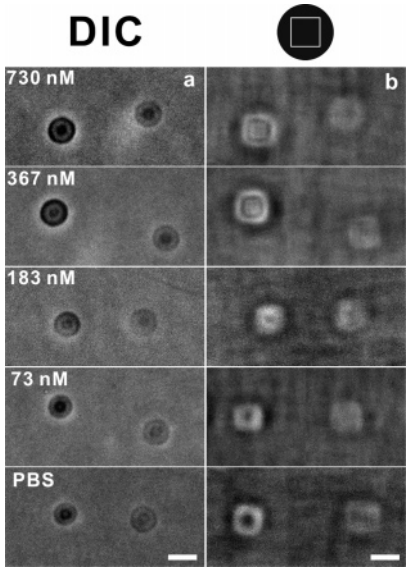

Figure 5. Influence of polyclonal anti-biotin on the hydrogel microlenses in 10 mM PBS buffer solution as a function of anti-biotin concentration at room temperature. (a) DIC microscopy images of bare microgels (right element in each panel) and biotinylated microgels (left element in each panel) at the indicated anti-biotin concentrations. (b) Projection of the single square pattern (top right) through the hydrogel microlenses under the same conditions as described for column a. As the anti-biotin concentration increases, only the biotinylated hydrogel microlenses form dark circles in DIC images (a) and tightly focused square images in projection mode (b). Note that 150 μL of each solution was used for this experiment (367 nM is equivalent to 55 pmol). The scale bar is 2 μm.

low dissociation constant (and hence small dissociation rate constant) of the biotin:avidin pair ($K_d \sim 10^{-13}-10^{-15}$), the free biotin is not expected to exchange with the hydrogel-bound biotin on the time scale of the experiments. Thus, this experiment allows for a measure of avidin-based cross-linking as a function of the number of free binding sites. Comparing the data in Figure 3 with those in Figure 1, where free avidin is used, suggests that the hydrogel microlens is less sensitive to avidin that has been pre-equilibrated with biotin than with free avidin. In the case of 1:1 biotin:avidin, the microlens is observed to "turn on" at ~200 nM (30 pmol of avidin), while for 2:1 biotin:avidin, the lens is not switched until ~600 nM (90 pmol of avidin). This behavior can be reasonably understood by the fact that the free avidin statistically will have more opportunities to form cross-links than avidin with partially occupied binding sites. To eliminate the possibility that the focal length change is caused by monovalent binding and/or nonspecific binding of avidin, we exposed microlens arrays to solutions of avidin pre-equilibrated with 3 (monovalent avidin) and 5 (excess biotin) equiv of biotin (Figure 4). Under these conditions, we observe no discernible change in lens focal length due to the statistical improbability of protein-based cross-linking under conditions where one or fewer binding sites is available on the protein.

To evaluate the generality of the assay for protein detection, we investigated a weaker binding protein−ligand interaction. In this case, a polyclonal antiserum (IgG fraction) raised in goat against biotin was used as the cross-linking protein. Note that an IgG is different from avidin in a number of ways. It has a higher molecular weight (~150 kDa vs ~66 kDa for avidin), it has only two binding sites (paratopes) for biotin, and it is expected to have a much higher dissociation constant than that of avidin. Typical effective (ensemble) dissociation constants for polyclonal antisera are on the order of $K_d \sim 10^{-9}$ M. Panels a and b of Figure 5 show the DIC images and the projected pattern images as a function of anti-biotin concentration, respectively. The hydrogel microlens assay displays a focal length change at a concentration above 367 nM (equivalent to 55 pmol), with the general microlens appearance being very similar to that observed for avidin binding. If one compares Figure 3c,d with Figure 5a,b, where the effective number of binding sites to biotin is the same but the K_d values are different, we find that the microlens assay is more sensitive to anti-biotin than it is to avidin, despite avidin's lower K_d value. While it is possible that this arises from the higher molecular weight of the IgG, it is also reasonable to consider the larger distance between binding sites in the IgG. It may be the case that the IgG is statistically a better cross-linker simply because it can access more biotins than the smaller avidin. Also, it should be pointed out that the anti-biotin assay is less sensitive than the avidin assay in Figure 3a,b, where the avidin has three active binding sites. Thus, the sensitivity of the cross-linking assay will be due to the protein:ligand affinity, the number of ligand binding sites, and the distance between binding sites on the protein.

The reversibility of the hydrogel microlens assay is shown in Figure 6. The hydrogel microlenses were stepwise exposed to PBS buffer (row a), polyclonal anti-biotin solution (row b), and biotin solution (rows c and d). As shown, when the antibody-bound microlenses are exposed to a solution of the free ligand, the focal length of the microlens reverts back to its original state, suggesting that the protein-based cross-links have been disrupted. This result suggests that this construct could potentially be used in a displacement-type assay. For example, each microlens could contain both a tethered protein and a tethered ligand, where association between the two results in a cross-linking point and, hence, a decrease in focal length. However, upon exposure to the free ligand or protein (depending on what is to be assayed), these cross-links would be disrupted, thereby increasing the lens focal length, which can be visualized on a simple optical microscope. A displacement assay of this type would have the advantage of being reversible since the displaced moiety would remain tethered to the microlens. Following washing, the protein:ligand cross-link would be re-

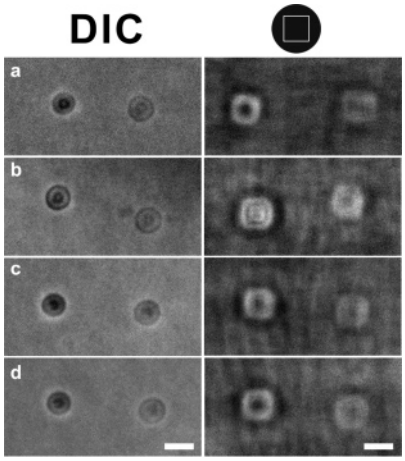

Figure 6. Reversibility of the hydrogel microlens assay. (Left column) DIC images of the hydrogel microlenses and (right column) projected square pattern images through the hydrogel microlenses. The hydrogel microlenses were stepwise exposed to 10 mM PBS buffer (row a), 667 nM polyclonal anti-biotin solution (row b), and 1 mM free biotin solution (row c after 3 h and (d) after 22 h). The bare microgels are the right elements in each panel, and biotinylated microgels are the left elements in each panel. Note that 150 μL of each solution was used for this experiment (667 nM is equivalent to 100 pmol). The scale bar is 2 μm.

formed, thereby resetting the microlens to the "on" state. Furthermore, if one were able to tune either the dissociation constant of the tethered protein:ligand pair or the critical number of cross-links required for microlens modulation, the sensitivity of the assay to the solution concentration of analyte could be tuned to a level appropriate for a particular application.

In conclusion, we have demonstrated that biotin-functionalized hydrogel microlenses can be used to assay avidin and polyclonal anti-biotin using a brightfield optical microscopy technique. The hydrogel microlens assay can be easily constructed in inexpensive, simple, and rapid fashion, with high selectivity. The unique characteristics of the assay technology include the ability to determine the presence of an expected protein by monitoring the focal length of the microlens without the need for covalent tagging of the protein of interest. Furthermore, these microlenses could individually represent pixels in a biochip-type format, where such a chip could be read-out by simple optical microscopy coupled with image recognition software, again in a label-free format. These fundamental advantages make this new technique attractive for the future development of a displacement-type protein assay, where "on" and "off" signals are sufficient for primary affinity screening. However, it should be noted that the present materials platform represents a nonoptimized format for biological sensing, as the polymers used here may be overly sensitive to changes in ionic strength in the physiological range and will certainly be sensitive to changes in ambient temperature. Thus, we have demonstrated the first major steps toward practically applicable bioresponsive materials, with further optimization required before true applications result.

Acknowledgment. L.A.L. acknowledges financial support from a Sloan Fellowship and a Camille Dreyfus Teacher-Scholar Award. We thank Prof. J. Fourkas (University of Maryland) for helpful discussions during the course of this work.

Supporting Information Available: Supplementary images of microlenses shown in Figures 1, 2, and 5, and the Experimental Section. This material is available free of charge via the Internet at http://pubs.acs.org.

JA0519076